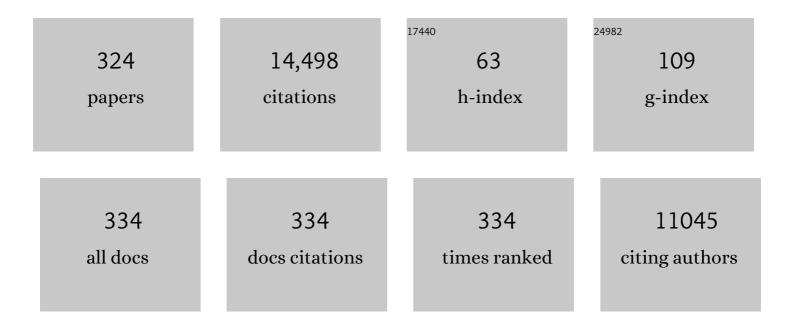
List of Publications by Year in descending order

Source: https://exaly.com/author-pdf/2580218/publications.pdf Version: 2024-02-01



#	Article	IF	CITATIONS
1	Effects of Lipid Lowering by Pravastatin on Progression and Regression of Coronary Artery Disease in Symptomatic Men With Normal to Moderately Elevated Serum Cholesterol Levels. Circulation, 1995, 91, 2528-2540.	1.6	718
2	Diet, Lipoproteins, and the Progression of Coronary Atherosclerosis. New England Journal of Medicine, 1985, 312, 805-811.	27.0	512
3	Infarct Tissue Heterogeneity Assessed With Contrast-Enhanced MRI Predicts Spontaneous Ventricular Arrhythmia in Patients With Ischemic Cardiomyopathy and Implantable Cardioverter-Defibrillator. Circulation: Cardiovascular Imaging, 2009, 2, 183-190.	2.6	406
4	Diagnostic Accuracy of Fast Computational Approaches to DeriveÂFractional Flow Reserve FromÂDiagnostic Coronary Angiography. JACC: Cardiovascular Interventions, 2016, 9, 2024-2035.	2.9	394
5	3-D active appearance models: segmentation of cardiac MR and ultrasound images. IEEE Transactions on Medical Imaging, 2002, 21, 1167-1178.	8.9	348
6	Fractional Flow Reserve Calculation From 3-Dimensional Quantitative Coronary AngiographyÂand TIMI Frame Count. JACC: Cardiovascular Interventions, 2014, 7, 768-777.	2.9	292
7	Assessment of percutaneous transluminal coronary angioplasty by quantitative coronary angiography: Diameter versus densitometric area measurements. American Journal of Cardiology, 1984, 54, 482-488.	1.6	272
8	Automatic segmentation of echocardiographic sequences by active appearance motion models. IEEE Transactions on Medical Imaging, 2002, 21, 1374-1383.	8.9	257
9	Comparison of echocardiographic methods with magnetic resonance imaging for assessment of right ventricular function in children. American Journal of Cardiology, 1995, 76, 589-594.	1.6	250
10	LDL-Apheresis Atherosclerosis Regression Study (LAARS). Circulation, 1996, 93, 1826-1835.	1.6	239
11	Coronary Artery Dimensions from Cineangiograms-Methodology and Validation of a Computer-Assisted Analysis Procedure. IEEE Transactions on Medical Imaging, 1984, 3, 131-141.	8.9	238
12	Evaluation of plaque characteristics in acute coronary syndromes: non-invasive assessment with multi-slice computed tomography and invasive evaluation with intravascular ultrasound radiofrequency data analysis. European Heart Journal, 2008, 29, 2373-2381.	2.2	215
13	Comparison Between Manual and Semiautomated Analysis of Left Ventricular Volume Parameters from Short-Axis MR Images. Journal of Computer Assisted Tomography, 1997, 21, 756-765.	0.9	198
14	SPASM: A 3D-ASM for segmentation of sparse and arbitrarily oriented cardiac MRI data. Medical Image Analysis, 2006, 10, 286-303.	11.6	194
15	Automated quantification of coronary plaque with computed tomography: comparison with intravascular ultrasound using a dedicated registration algorithm for fusion-based quantification. European Heart Journal, 2012, 33, 1007-1016.	2.2	194
16	Head-to-head comparison of contrast-enhanced magnetic resonance imaging and electroanatomical voltage mapping to assess post-infarct scar characteristics in patients with ventricular tachycardias: real-time image integration and reversed registration. European Heart Journal, 2011, 32, 104-114.	2.2	193
17	A new approach for the quantification of complex lesion morphology: The gradient field transform; Basic principles and validation results. Journal of the American College of Cardiology, 1994, 24, 216-224.	2.8	184
18	Automatic quantification and characterization of coronary atherosclerosis with computed tomography coronary angiography: cross-correlation with intravascular ultrasound virtual histology. International Journal of Cardiovascular Imaging, 2013, 29, 1177-1190.	1.5	178

#	Article	IF	CITATIONS
19	Hierarchical functional modularity in the restingâ€state human brain. Human Brain Mapping, 2009, 30, 2220-2231.	3.6	174
20	Quantification of right ventricular function with magnetic resonance imaging in children with normal hearts and with congenital heart disease. American Heart Journal, 1995, 130, 828-837.	2.7	173
21	Mitral Valve and Tricuspid Valve Blood Flow: Accurate Quantification with 3D Velocity-encoded MR Imaging with Retrospective Valve Tracking. Radiology, 2008, 249, 792-800.	7.3	160
22	Evaluation of Coronary Artery Stenosis by Quantitative Flow Ratio During Invasive Coronary Angiography. Circulation: Cardiovascular Imaging, 2018, 11, e007107.	2.6	157
23	Accuracy and precision of quantitative digital coronary arteriography: Observerâ€, shortâ€, and mediumâ€term variabilities. Catheterization and Cardiovascular Diagnosis, 1993, 28, 187-198.	0.3	152
24	Early detection of restenosis after successful percutaneous transluminal coronary angioplasty by exercise-redistribution thallium scintigraphy. American Journal of Cardiology, 1985, 55, 357-361.	1.6	142
25	Detection and Quantification of Dysfunctional Myocardium by Magnetic Resonance Imaging. Circulation, 1997, 95, 924-931.	1.6	142
26	Reproducibility of total cerebral blood flow measurements using phase contrast magnetic resonance imaging. Journal of Magnetic Resonance Imaging, 2002, 16, 1-5.	3.4	138
27	Impact of Simultaneous Pancreas and Kidney Transplantation on Progression of Coronary Atherosclerosis in Patients With End-Stage Renal Failure due to Type 1 Diabetes. Diabetes Care, 2002, 25, 906-911.	8.6	128
28	Assessment of Left Ventricular Dyssynchrony in Patients With Conduction Delay and Idiopathic Dilated Cardiomyopathy. Journal of the American College of Cardiology, 2006, 47, 2042-2048.	2.8	128
29	Automatic centerline extraction of coronary arteries in coronary computed tomographic angiography. International Journal of Cardiovascular Imaging, 2012, 28, 921-933.	1.5	127
30	Quantitative assessment of regional left ventricular motion using endocardial landmarks. Journal of the American College of Cardiology, 1986, 7, 317-326.	2.8	123
31	Flow Assessment Through Four Heart Valves Simultaneously Using 3-Dimensional 3-Directional Velocity-Encoded Magnetic Resonance Imaging With Retrospective Valve Tracking in Healthy Volunteers and Patients With Valvular Regurgitation. Investigative Radiology, 2009, 44, 669-675.	6.2	121
32	Diagnostic performance of angiography-derived fractional flow reserve: a systematic review and Bayesian meta-analysis. European Heart Journal, 2018, 39, 3314-3321.	2.2	116
33	Automated Measurement of Volume Flow in the Ascending Aorta Using MR Velocity Maps. Journal of Computer Assisted Tomography, 1998, 22, 904-911.	0.9	115
34	Comparison of Clinical Interpretation With Visual Assessment and Quantitative Coronary Angiography in Patients Undergoing Percutaneous Coronary Intervention in Contemporary Practice. Circulation, 2013, 127, 1793-1800.	1.6	114
35	In-vivo validation of on-line and off-line geometric coronary measurements using insertion of stenosis phantoms in porcine coronary arteries. Catheterization and Cardiovascular Diagnosis, 1992, 27, 16-27.	0.3	112
36	The Asp <sub>9</sub> Asn Mutation in the Lipoprotein Lipase Gene Is Associated With Increased Progression of Coronary Atherosclerosis. Circulation, 1996, 94, 1913-1918.	1.6	103

#	Article	IF	CITATIONS
37	Shape differences of the brain ventricles in Alzheimer's disease. NeuroImage, 2006, 32, 1060-1069.	4.2	102
38	In vivo comparison of arterial lumen dimensions assessed by co-registered three-dimensional (3D) quantitative coronary angiography, intravascular ultrasound and optical coherence tomography. International Journal of Cardiovascular Imaging, 2012, 28, 1315-1327.	1.5	97
39	Fast and accurate automated measurements in digitized stereophotogrammetric radiographs. Journal of Biomechanics, 1998, 31, 491-498.	2.1	95
40	Heparin -coated Wiktor stents in human coronary arteries (MENTOR Trial). American Journal of Cardiology, 2000, 86, 385-389.	1.6	94
41	Effect of pravastatin on progression and regression of coronary atherosclerosis and vessel wall changes in carotid and femoral arteries: A report from the regression growth evaluation statin study. American Journal of Cardiology, 1995, 76, 40C-46C.	1.6	90
42	Comprehensive assessment of spotty calcifications on computed tomography angiography: Comparison to plaque characteristics on intravascular ultrasound with radiofrequency backscatter analysis. Journal of Nuclear Cardiology, 2011, 18, 893-903.	2.1	90
43	Assessment of dimensions and image quality of coronary contrast catheters from cineangiograms. Catheterization and Cardiovascular Diagnosis, 1985, 11, 521-531.	0.3	88
44	Atlas-based whole-body segmentation of mice from low-contrast Micro-CT data. Medical Image Analysis, 2010, 14, 723-737.	11.6	84
45	Biomechanical Modeling to Improve Coronary Artery Bifurcation Stenting. JACC: Cardiovascular Interventions, 2015, 8, 1281-1296.	2.9	84
46	Change in diameter of coronary artery segments adjacent to stenosis after percutaneous transluminal coronary angioplasty: Failure of percent diameter stenosis measurement to reflect morphologic changes induced by balloon dilation. Journal of the American College of Cardiology, 1988, 12, 315-323.	2.8	81
47	Which Cineangiographically Assessed Anatomic Variable Correlates Best With Functional Measurements of Stenosis Severity? A Comparison of Quantitative Analysis of the Coronary Cineangiogram with Measured Coronary Flow Reserve and Exercise/Redistribution Thallium-201 Scintigraphy. Journal of the American College of Cardiology, 1988, 12, 686-691.	2.8	81
48	Echo Planar MRI of the Heart on a Standard System: Validation of Measurements of Left Ventricular Function and Mass. Journal of Computer Assisted Tomography, 1996, 20, 942-949.	0.9	81
49	Quantitative Flow Ratio Identifies Nonculprit Coronary Lesions Requiring Revascularization in Patients With ST-Segment–Elevation Myocardial Infarction and Multivessel Disease. Circulation: Cardiovascular Interventions, 2018, 11, e006023.	3.9	80
50	Variability in Densitometric Assessment of Pulmonary Emphysema With Computed Tomography. Investigative Radiology, 2005, 40, 777-783.	6.2	79
51	Fully Automated Motion Correction in First-Pass Myocardial Perfusion MR Image Sequences. IEEE Transactions on Medical Imaging, 2008, 27, 1611-1621.	8.9	79
52	Evidence for a Synergistic Effect of Calcium Channel Blockers With Lipid-Lowering Therapy in Retarding Progression of Coronary Atherosclerosis in Symptomatic Patients With Normal to Moderately Raised Cholesterol Levels. Arteriosclerosis, Thrombosis, and Vascular Biology, 1996, 16, 425-430.	2.4	78
53	Quantitative analysis of cardiovascular MR images. International Journal of Cardiovascular Imaging, 1997, 13, 247-258.	0.6	78
54	Automated Detection of Regional Wall Motion Abnormalities Based on a Statistical Model Applied to Multislice Short-Axis Cardiac MR Images. IEEE Transactions on Medical Imaging, 2009, 28, 595-607.	8.9	77

#	Article	IF	CITATIONS
55	Anatomic Considerations of Cochlear Morphology and Its Implications for Insertion Trauma in Cochlear Implant Surgery. Otology and Neurotology, 2009, 30, 471-477.	1.3	75
56	Impact of Side Branch Modeling on Computation of Endothelial Shear Stress in Coronary Artery Disease. Journal of the American College of Cardiology, 2015, 66, 125-135.	2.8	75
57	A 3-D Active Shape Model Driven by Fuzzy Inference: Application to Cardiac CT and MR. IEEE Transactions on Information Technology in Biomedicine, 2008, 12, 595-605.	3.2	74
58	Repeatability of Lung Density Measurements with Low-Dose Computed Tomography in Subjects with α-1-Antitrypsin Deficiency–Associated Emphysema. Investigative Radiology, 2001, 36, 648-651.	6.2	73
59	Automated segmentation of myocardial scar in late enhancement MRI using combined intensity and spatial information. Magnetic Resonance in Medicine, 2010, 64, 586-594.	3.0	71
60	Clinical Implication of Quantitative Flow Ratio After Percutaneous Coronary Intervention for 3-Vessel Disease. JACC: Cardiovascular Interventions, 2019, 12, 2064-2075.	2.9	71
61	Positive Remodeling on Coronary Computed Tomography as a Marker for Plaque Vulnerability on Virtual Histology Intravascular Ultrasound. American Journal of Cardiology, 2011, 107, 1725-1729.	1.6	69
62	Fractional flow reserve in clinical practice: from wire-based invasive measurement to image-based computation. European Heart Journal, 2020, 41, 3271-3279.	2.2	69
63	Operator Induced Variability in Cardiovascular MR: Left Ventricular Measurements and Their Reproducibility. Journal of Cardiovascular Magnetic Resonance, 2005, 7, 447-457.	3.3	68
64	Fusion of 3D QCA and IVUS/OCT. International Journal of Cardiovascular Imaging, 2011, 27, 197-207.	1.5	66
65	Sources of Error in Lung Densitometry with CT. Investigative Radiology, 1999, 34, 303.	6.2	66
66	Results of the first clinical study of adjunctive CAldaret (MCC-135) in patients undergoing primary percutaneous coronary intervention for ST-Elevation Myocardial Infarction: the randomized multicentre CASTEMI study. European Heart Journal, 2006, 27, 2516-2523.	2.2	63
67	A strain energy filter for 3D vessel enhancement with application to pulmonary CT images. Medical Image Analysis, 2011, 15, 112-124.	11.6	62
68	The use of Roentgen stereophotogrammetry to study micromotion of orthopaedic implants. ISPRS Journal of Photogrammetry and Remote Sensing, 2002, 56, 376-389.	11.1	61
69	Time Continuous Tracking and Segmentation of Cardiovascular Magnetic Resonance Images Using Multidimensional Dynamic Programming. Investigative Radiology, 2006, 41, 52-62.	6.2	61
70	Edge detection versus densitometry in the quantitative assessment of stenosis phantoms: An in vivo comparison in porcine coronary arteries. American Heart Journal, 1992, 124, 1181-1189.	2.7	57
71	Advanced contour detection for three-dimensional intracoronary ultrasound: a validation–in vitro and in vivo. International Journal of Cardiovascular Imaging, 2002, 18, 235-248.	0.6	57
72	Quantitative analysis of regional left ventricular function after myocardial infarction in the pig assessed with cine magnetic resonance imaging. Magnetic Resonance in Medicine, 1995, 34, 161-169.	3.0	56

#	Article	IF	CITATIONS
73	Vessel diameter measurements in gadolinium contrast-enhanced three-dimensional MRA of peripheral arteries. Magnetic Resonance Imaging, 2000, 18, 13-22.	1.8	56
74	Automated Quantification of Stenosis Severity on 64-Slice CT. JACC: Cardiovascular Imaging, 2010, 3, 699-709.	5.3	56
75	Diagnostic performance of 320-slice multidetector computed tomography coronary angiography in patients after coronary artery bypass grafting. European Radiology, 2011, 21, 2285-2296.	4.5	55
76	Accurate and reproducible reconstruction of coronary arteries and endothelial shear stress calculation using 3D OCT: Comparative study to 3D IVUS and 3D QCA. Atherosclerosis, 2015, 240, 510-519.	0.8	55
77	In vivo assessment of bifurcation optimal viewing angles and bifurcation angles by three-dimensional (3D) quantitative coronary angiography. International Journal of Cardiovascular Imaging, 2012, 28, 1617-1625.	1.5	54
78	Comparison of the Sensitivities of 5 Different Computed Tomography Scanners for the Assessment of the Progression of Pulmonary Emphysema. Investigative Radiology, 2004, 39, 1-7.	6.2	52
79	Ultrasound Assessment of Atherosclerotic Vessel Wall Changes. Investigative Radiology, 2000, 35, 699-706.	6.2	51
80	Evaluation of a New Method for Automated Detection of Left Ventricular Boundaries in Time Series of Magnetic Resonance Images Using an Active Appearance Motion Model. Journal of Cardiovascular Magnetic Resonance, 2004, 6, 609-617.	3.3	50
81	The Influence of Flow, Vessel Diameter, and Non-Newtonian Blood Viscosity on the Wall Shear Stress in a Carotid Bifurcation Model for Unsteady Flow. Investigative Radiology, 2005, 40, 277-294.	6.2	50
82	Edge detection versus densitometry for assessing coronary stenting quantitatively. American Journal of Cardiology, 1991, 67, 484-490.	1.6	49
83	Ventricular shape biomarkers for Alzheimer's disease in clinical MR images. Magnetic Resonance in Medicine, 2008, 59, 260-267.	3.0	49
84	Fractional Flow Reserve and Coronary Bifurcation Anatomy. JACC: Cardiovascular Interventions, 2015, 8, 564-574.	2.9	49
85	Morphological Hippocampal Markers for Automated Detection of Alzheimer's Disease and Mild Cognitive Impairment Converters in Magnetic Resonance Images. Journal of Alzheimer's Disease, 2009, 17, 643-659.	2.6	48
86	Automatic stent strut detection in intravascular optical coherence tomographic pullback runs. International Journal of Cardiovascular Imaging, 2013, 29, 29-38.	1.5	48
87	Feasibility of Diastolic Function Assessment With Cardiac CT. JACC: Cardiovascular Imaging, 2011, 4, 246-256.	5.3	47
88	Ageâ€related and regional changes of aortic stiffness in the marfan syndrome: Assessment with velocityâ€encoded MRI. Journal of Magnetic Resonance Imaging, 2011, 34, 526-531.	3.4	47
89	Progression and regression of human coronary atherosclerosis The role of lipoproteins, lipases and thyroid hormones in coronary lesion growth. Atherosclerosis, 1987, 68, 51-58.	0.8	44
90	MMSE scores correlate with local ventricular enlargement in the spectrum from cognitively normal to Alzheimer disease. NeuroImage, 2008, 39, 1832-1838.	4.2	44

#	Article	IF	CITATIONS
91	Improved aortic pulse wave velocity assessment from multislice twoâ€directional inâ€plane velocityâ€encoded magnetic resonance imaging. Journal of Magnetic Resonance Imaging, 2010, 32, 1086-1094.	3.4	44
92	Automatic lumen and outer wall segmentation of the carotid artery using deformable threeâ€dimensional models in MR angiography and vessel wall images. Journal of Magnetic Resonance Imaging, 2012, 35, 156-165.	3.4	44
93	A novel method to assess coronary artery bifurcations by OCT: cut-plane analysis for side-branch ostial assessment from a main-vessel pullback. European Heart Journal Cardiovascular Imaging, 2015, 16, 177-189.	1.2	44
94	Towards quantitative analysis of coronary CTA. International Journal of Cardiovascular Imaging, 2005, 21, 73-84.	1.5	43
95	Feasibility study on automated recognition of allergenic pollen: grass, birch and mugwort. Aerobiologia, 2006, 22, 275-284.	1.7	43
96	7T T2â^—-weighted magnetic resonance imaging reveals cortical phase differences between early- and late-onset Alzheimer's disease. Neurobiology of Aging, 2015, 36, 20-26.	3.1	43
97	Predictors of coronary in-stent restenosis: importance of angiotensin-converting enzyme gene polymorphism and treatment with angiotensin-converting enzyme inhibitors. Journal of the American College of Cardiology, 2001, 38, 1434-1439.	2.8	42
98	A novel threeâ€dimensional quantitative coronary angiography system: Inâ€vivo comparison with intravascular ultrasound for assessing arterial segment length. Catheterization and Cardiovascular Interventions, 2010, 76, 291-298.	1.7	42
99	MRI-assessed regional pulse wave velocity for predicting absence of regional aorta luminal growth in marfan syndrome. International Journal of Cardiology, 2013, 167, 2977-2982.	1.7	41
100	Co-registration of optical coherence tomography and X-ray angiography in percutaneous coronary intervention. The Does Optical Coherence Tomography Optimize Revascularization (DOCTOR) fusion study. International Journal of Cardiology, 2015, 182, 272-278.	1.7	41
101	Angiotensin-Converting Enzyme Inhibitor Therapy Affects Left Ventricular Mass in Patients With Ejection Fraction >40% After Acute Myocardial Infarction. Journal of the American College of Cardiology, 1997, 29, 49-54.	2.8	39
102	Automated Observer-independent Acquisition of Cardiac Short-Axis MR Images: A Pilot Study. Radiology, 2001, 221, 537-542.	7.3	39
103	GAMEs: Growing and adaptive meshes for fully automatic shape modeling and analysis. Medical Image Analysis, 2007, 11, 302-314.	11.6	39
104	Reperfusion ventricular arrhythmia 'bursts' predict larger infarct size despite TIMI 3 flow restoration with primary angioplasty for anterior ST-elevation myocardial infarction. European Heart Journal, 2008, 30, 757-764.	2.2	39
105	Shape Abnormalities of the Striatum in Alzheimer's Disease. Journal of Alzheimer's Disease, 2011, 23, 49-59.	2.6	39
106	Assessment of obstruction length and optimal viewing angle from biplane X-ray angiograms. International Journal of Cardiovascular Imaging, 2010, 26, 5-17.	1.5	37
107	Automatic detection of bioresorbable vascular scaffold struts in intravascular optical coherence tomography pullback runs. Biomedical Optics Express, 2014, 5, 3589.	2.9	37
108	ST elevation acute myocardial infarction accelerates non-culprit coronary lesion atherosclerosis. International Journal of Cardiovascular Imaging, 2014, 30, 253-261.	1.5	37

#	Article	IF	CITATIONS
109	Quantitative analysis of left ventricular function from equilibrium gated blood pool scintigrams: an overview of computer methods. European Journal of Nuclear Medicine and Molecular Imaging, 1985, 10-10, 97-110.	2.1	36
110	Automatic vessel wall contour detection and quantification of wall thickness in in-vivo MR images of the human aorta. Journal of Magnetic Resonance Imaging, 2006, 24, 595-602.	3.4	36
111	Detection of areas with viable remnant tumor in postchemotherapy patients with Ewing's sarcoma by dynamic contrast-enhanced MRI using pharmacokinetic modeling. Magnetic Resonance Imaging, 2000, 18, 525-535.	1.8	35
112	Comparison of the Relation Between the Calcium Score and Plaque Characteristics in Patients With Acute Coronary Syndrome Versus Patients With Stable Coronary Artery Disease, Assessed by Computed Tomography Angiography and Virtual Histology Intravascular Ultrasound. American Journal of Cardiology, 2011, 108, 658-664.	1.6	35
113	Assessment of Regional Left Ventricular Wall Parameters from Short Axis Magnetic Resonance Imaging using a Three-Dimensional Extension to the Improved Centerline Method. Investigative Radiology, 1997, 32, 529-539.	6.2	35
114	Quantitative angiography methods for bifurcation lesions: a consensus statement update from the European Bifurcation Club. EuroIntervention, 2017, 13, 115-123.	3.2	35
115	Computer-aided diagnosis via model-based shape analysis. Academic Radiology, 2005, 12, 358-367.	2.5	34
116	Reperfusion ventricular arrhythmia 'bursts' in TIMI 3 flow restoration with primary angioplasty for anterior ST-elevation myocardial infarction: a more precise definition of reperfusion arrhythmias. Europace, 2008, 10, 988-997.	1.7	34
117	Detection of pollen grains in multifocal optical microscopy images of air samples. Microscopy Research and Technique, 2009, 72, 424-430.	2.2	34
118	Assessment With Multi-Slice Computed Tomography and Gray-Scale and Virtual Histology Intravascular Ultrasound of Gender-Specific Differences in Extent and Composition of Coronary Atherosclerotic Plaques in Relation to Age. American Journal of Cardiology, 2010, 105, 480-486.	1.6	34
119	Cardiac MR perfusion image processing techniques: A survey. Medical Image Analysis, 2012, 16, 767-785.	11.6	33
120	An Integrated Automated Analysis Method for Quantifying Vessel Stenosis and Plaque Burden From Carotid MRI Images. Stroke, 2006, 37, 2162-2164.	2.0	32
121	Automatic detection and quantification of the Agatston coronary artery calcium score on contrast computed tomography angiography. International Journal of Cardiovascular Imaging, 2015, 31, 151-161.	1.5	32
122	Accurate quantitation of regurgitant volume with MRI in patients selected for mitral valve repair. European Journal of Cardio-thoracic Surgery, 2005, 27, 462-467.	1.4	31
123	Cross-sectional, prospective study of MRI reproducibility in the assessment of plaque burden of the carotid arteries and aorta. Nature Reviews Cardiology, 2009, 6, 219-228.	13.7	31
124	Myocardial perfusion-fibrosis pattern in systemic sclerosis assessed by cardiac magnetic resonance. International Journal of Cardiology, 2012, 159, e56-e58.	1.7	31
125	Assessment of the Progression of Emphysema by Quantitative Analysis of Spirometrically Gated Computed Tomography Images. Investigative Radiology, 1996, 31, 761-767.	6.2	31
126	Catheter sizes for quantitative coronary arteriography. Catheterization and Cardiovascular Diagnosis, 1994, 33, 153-155.	0.3	30

#	Article	IF	CITATIONS
127	Accurate and Reproducible Mitral Valvular Blood Flow Measurement with Three?Directional Velocity?Encoded Magnetic Resonance Imaging. Journal of Cardiovascular Magnetic Resonance, 2004, 6, 767-776.	3.3	30
128	Quantitative Analysis of Computed Tomography Scans of the Lungs for the Diagnosis of Pulmonary Emphysema. Investigative Radiology, 1995, 30, 552-562.	6.2	29
129	Automated contour detection in X-ray left ventricular angiograms using multiview active appearance models and dynamic programming. IEEE Transactions on Medical Imaging, 2006, 25, 1158-1171.	8.9	29
130	Echogenicity as a surrogate for bioresorbable everolimus-eluting scaffold degradation: analysis at 1-, 3-, 6-, 12- 18, 24-, 30-, 36- and 42-month follow-up in a porcine model. International Journal of Cardiovascular Imaging, 2015, 31, 471-482.	1.5	29
131	Automatic identification of coronary tree anatomy in coronary computed tomography angiography. International Journal of Cardiovascular Imaging, 2017, 33, 1809-1819.	1.5	29
132	Magnetic resonance angiography of dialysis access shunts: Initial results. Magnetic Resonance Imaging, 1996, 14, 197-200.	1.8	28
133	Automated Tracking of the Mitral Valve Annulus Motion in Apical Echocardiographic Images Using Multidimensional Dynamic Programming. Ultrasound in Medicine and Biology, 2007, 33, 1389-1399.	1.5	28
134	New approaches for the assessment of vessel sizes in quantitative (cardio-)vascular X-ray analysis. International Journal of Cardiovascular Imaging, 2010, 26, 259-271.	1.5	28
135	Noninvasive Prediction of Atherosclerotic Progression: The PROSPECT-MSCT Study. JACC: Cardiovascular Imaging, 2016, 9, 1009-1011.	5.3	27
136	Randomized, controlled trial of secondary prevention of coronary sclerosis in normocholesterolemic patients using pravastatin: final 5-year angiographic follow-up of the Prevention of Coronary Sclerosis (PCS) study. International Journal of Cardiology, 2004, 97, 107-114.	1.7	26
137	New approach to quantitative angiographic assessment after stent implantation. , 1997, 40, 343-347.		25
138	Scan optimization of gadolinium contrast-enhanced three-dimensional MRA of peripheral arteries with multiple bolus injections and in vitro validation of stenosis quantification. Magnetic Resonance Imaging, 1999, 17, 47-57.	1.8	25
139	Toward Magnetic Resonanceâ€Guided Electroanatomical Voltage Mapping for Catheter Ablation of Scarâ€Related Ventricular Tachycardia: A Comparison of Registration Methods. Journal of Cardiovascular Electrophysiology, 2012, 23, 74-80.	1.7	25
140	In Vivo Flow Simulation at Coronary Bifurcation Reconstructed by Fusion of 3-Dimensional X-ray Angiography and Optical Coherence Tomography. Circulation: Cardiovascular Interventions, 2013, 6, e15-7.	3.9	25
141	Feasibility of an Automated Quantitative Computed Tomography Angiography–Derived Risk Score for Risk Stratification of Patients With Suspected Coronary Artery Disease. American Journal of Cardiology, 2014, 113, 1947-1955.	1.6	25
142	Automated and Accurate Assessment of the Distribution, Magnitude, and Direction of Pincushion Distortion in Angiographic Images. Investigative Radiology, 1995, 30, 204-213.	6.2	24
143	Automatic Model-Based Contour Detection and Blood Flow Quantification in Small Vessels with Velocity Encoded Magnetic Resonance Imaging. Investigative Radiology, 2003, 38, 567-577.	6.2	24
144	Left Ventricular Volume Estimation in Cardiac Three-dimensional Ultrasound. Academic Radiology, 2005, 12, 1241-1249.	2.5	24

#	Article	IF	CITATIONS
145	Sparse Registration for Three-Dimensional Stress Echocardiography. IEEE Transactions on Medical Imaging, 2008, 27, 1568-1579.	8.9	24
146	Total coronary atherosclerotic plaque burden assessment by CT angiography for detecting obstructive coronary artery disease associated with myocardial perfusion abnormalities. Journal of Cardiovascular Computed Tomography, 2016, 10, 121-127.	1.3	24
147	American College of Cardiology/ European Society of Cardiology international study of angiographic data compression phase II. Journal of the American College of Cardiology, 2000, 35, 1380-1387.	2.8	23
148	One core laboratory at two international sites, is that feasible? An inter-core laboratory and intra-observer variability study. Catheterization and Cardiovascular Interventions, 2002, 56, 333-340.	1.7	23
149	A novel approach for the detection of pathlines in X-ray angiograms: the wavefront propagation algorithm. International Journal of Cardiovascular Imaging, 2002, 18, 317-324.	0.6	22
150	Reproducibility of wall shear stress assessment with the paraboloid method in the internal carotid artery with velocity encoded MRI in healthy young individuals. Journal of Magnetic Resonance Imaging, 2007, 26, 598-605.	3.4	22
151	Dedicated bifurcation analysis: basic principles. International Journal of Cardiovascular Imaging, 2011, 27, 167-174.	1.5	22
152	Diastolic Carotid Artery Wall Shear Stress Is Associated With Cerebral Infarcts and Periventricular White Matter Lesions. Stroke, 2011, 42, 3497-3501.	2.0	22
153	Detection of coronary plaques using MR coronary vessel wall imaging: validation of findings with intravascular ultrasound. European Radiology, 2013, 23, 115-124.	4.5	22
154	Quantification of disturbed coronary flow by disturbed vorticity index and relation with fractional flow reserve. Atherosclerosis, 2018, 273, 136-144.	0.8	22
155	Pravastatin Decreases Wall Shear Stress and Blood Velocity in the Internal Carotid Artery Without Affecting Flow Volume. Stroke, 2007, 38, 1374-1376.	2.0	21
156	Magnetic resonance imaging assessment of reverse left ventricular remodeling late after restrictive mitral annuloplasty in early stages of dilated cardiomyopathy. Journal of Thoracic and Cardiovascular Surgery, 2008, 135, 1247-1253.	0.8	21
157	Associations between Magnetic Resonance Imaging Measures and Neuropsychological Impairment in Early and Late Onset Alzheimer's Disease. Journal of Alzheimer's Disease, 2013, 35, 169-178.	2.6	21
158	Variations in blood flow waveforms in stenotic renal arteries by 2D phase-contrast cine MRI. Journal of Magnetic Resonance Imaging, 1998, 8, 590-597.	3.4	20
159	The impact of acquisition angle differences on threeâ€dimensional quantitative coronary angiography. Catheterization and Cardiovascular Interventions, 2011, 78, 214-222.	1.7	20
160	Analyses of aerodynamic characteristics of the oropharynx applying CBCT: obstructive sleep apnea patients versus control subjects. Dentomaxillofacial Radiology, 2018, 47, 20170238.	2.7	20
161	Left ventricular wall motion analysis in patients with acute myocardial infarction using magnetic resonance imaging. Magnetic Resonance Imaging, 1993, 11, 485-492.	1.8	19
162	Hippocampal atrophy in people with memory deficits: results from the population-based IPREA study. International Psychogeriatrics, 2014, 26, 1067-1081.	1.0	19

#	Article	IF	CITATIONS
163	3D assessment of stent cell size and side branch access in intravascular optical coherence tomographic pullback runs. Computerized Medical Imaging and Graphics, 2014, 38, 113-122.	5.8	19
164	QCA, IVUS and OCT in interventional cardiology in 2011. Cardiovascular Diagnosis and Therapy, 2011, 1, 57-70.	1.7	19
165	Effect of data compression on quantitative coronary measurements. Catheterization and Cardiovascular Diagnosis, 1995, 34, 175-185.	0.3	18
166	Effect of lossy data compression on quantitative coronary measurements. International Journal of Cardiovascular Imaging, 1997, 13, 261-270.	0.6	18
167	Multiview Active Appearance Models for Simultaneous Segmentation of Cardiac 2- and 4-Chamber Long-Axis Magnetic Resonance Images. Investigative Radiology, 2005, 40, 195-203.	6.2	18
168	Fully Automatic Registration and Segmentation of First-Pass Myocardial Perfusion MR Image Sequences. Academic Radiology, 2010, 17, 1375-1385.	2.5	18
169	The Aging Imageomics Study: rationale, design and baseline characteristics of the study population. Mechanisms of Ageing and Development, 2020, 189, 111257.	4.6	18
170	A novel software tool for semi-automatic quantification of thoracic aorta dilatation on baseline and follow-up computed tomography angiography. International Journal of Cardiovascular Imaging, 2019, 35, 711-723.	1.5	17
171	Quantification of Global and Regional Ventricular Function in Cardiac Magnetic Resonance Imaging. Topics in Magnetic Resonance Imaging, 2000, 11, 348-358.	1.2	16
172	Model driven quantification of left ventricular function from sparse single-beat 3D echocardiography. Medical Image Analysis, 2010, 14, 582-593.	11.6	16
173	Comparisons of angiographic core laboratory analyses of phantom and clinical images: Interlaboratory variability. , 1996, 37, 24-31.		15
174	Anatomical Modeling with Fuzzy Implicit Surface Templates: Application to Automated Localization of the Heart and Lungs in Thoracic MR Volumes. Computer Vision and Image Understanding, 2000, 80, 1-20.	4.7	15
175	Automated quantification of carotid artery stenosis on contrast-enhanced MRA data using a deformable vascular tube model. International Journal of Cardiovascular Imaging, 2012, 28, 1513-1524.	1.5	15
176	Atrioventricular conduction in mammalian species: Hemodynamic and electrical scaling. Heart Rhythm, 2005, 2, 188-196.	0.7	14
177	The maximum necrotic core area is most often located proximally to the site of most severe narrowing: a virtual histology intravascular ultrasound study. Heart and Vessels, 2013, 28, 166-172.	1.2	14
178	The reproducibility of cardiac and liver T2* measurement in thalassemia major using two different software packages. International Journal of Cardiovascular Imaging, 2013, 29, 1511-1516.	1.5	14
179	The impact of image resolution on computation of fractional flow reserve: coronary computed tomography angiography versus 3-dimensional quantitative coronary angiography. International Journal of Cardiovascular Imaging, 2016, 32, 513-523.	1.5	14
180	Feature tracking computed tomography-derived left ventricular global longitudinal strain in patients with aortic stenosis: a comparative analysis with echocardiographic measurements. Journal of Cardiovascular Computed Tomography, 2020, 14, 240-245.	1.3	14

#	Article	IF	CITATIONS
181	A novel four-dimensional angiographic approach to assess dynamic superficial wall stress of coronary arteries in vivo: initial experience in evaluating vessel sites with subsequent plaque rupture. EuroIntervention, 2017, 13, e1099-e1103.	3.2	14
182	Gadolinium contrast-enhanced three-dimensional MRA of peripheral arteries with multiple bolus injection: scan optimization in vitro and in vivo. International Journal of Cardiovascular Imaging, 1999, 15, 161-173.	0.6	13
183	Automated Contour Detection in Cardiac MRI Using Active Appearance Models. Investigative Radiology, 2007, 42, 697-703.	6.2	13
184	First Presentation of 3-Dimensional Reconstruction and Centerline-Guided Assessment of Coronary Bifurcation by Fusion of X-Ray Angiography and Optical Coherence Tomography. JACC: Cardiovascular Interventions, 2012, 5, 884-885.	2.9	13
185	Evaluation of sampling density on the accuracy of aortic pulse wave velocity from velocityâ€encoded MRI in patients with Marfan syndrome. Journal of Magnetic Resonance Imaging, 2012, 36, 1470-1476.	3.4	13
186	Fully automated side branch detection in intravascular optical coherence tomography pullback runs. Biomedical Optics Express, 2014, 5, 3160.	2.9	13
187	Enhanced characterization of calcified areas in intravascular ultrasound virtual histology images by quantification of the acoustic shadow: validation against computed tomography coronary angiography. International Journal of Cardiovascular Imaging, 2016, 32, 543-552.	1.5	13
188	Comparison of Diagnostic Performance of Quantitative Flow Ratio in Patients With Versus Without Diabetes Mellitus. American Journal of Cardiology, 2019, 123, 1722-1728.	1.6	13
189	Computer analysis of moving radiopaque markers from X-ray cinefilms. Computer Graphics and Image Processing, 1979, 11, 35-48.	0.8	12
190	Standardization of Central Off-Line Quantitative Image Analysis: Implications from Experiences with Quantitative Coronary Angiography. Cardiology, 2001, 1, 44-51.	0.3	12
191	Effect of Caldaret on the Incidence of Severe Left Ventricular Dysfunction in Patients With ST-Elevation Myocardial Infarction Undergoing Primary Coronary Intervention. American Journal of Cardiology, 2009, 103, 1-4.	1.6	12
192	Quantification of aortic annulus in computed tomography angiography: Validation of a fully automatic methodology. European Journal of Radiology, 2017, 93, 1-8.	2.6	12
193	Invasive assessment of coronary artery disease. Journal of Nuclear Cardiology, 2018, 25, 860-871.	2.1	12
194	Stenting of long coronary artery lesions: Initial angiographic results and 6-month clinical outcome of the micro stent II-XL. Catheterization and Cardiovascular Interventions, 1999, 48, 105-112.	1.7	11
195	Quantitative Assessment of the Morphology of Renal Arteries from X-ray Images. Investigative Radiology, 2004, 39, 365-373.	6.2	11
196	Autonomous virtual mobile robot for three-dimensional medical image exploration: Application to micro-CT cochlear images. Artificial Intelligence in Medicine, 2008, 43, 1-15.	6.5	11
197	Is it safe to implant bioresorbable scaffolds in ostial side-branch lesions? Impact of â€~neo-carina' formation on main-branch flow pattern. Longitudinal clinical observations. Atherosclerosis, 2015, 238, 22-25.	0.8	11
198	Prognostic Influence of Feature Tracking Multidetector Row Computed Tomography-Derived Left Ventricular Global Longitudinal Strain in Patients with Aortic Stenosis Treated With Transcatheter Aortic Valve Implantation. American Journal of Cardiology, 2020, 125, 948-955.	1.6	11

#	Article	IF	CITATIONS
199	Usefulness of digital angiography in the assessment of left ventricular ejection fraction. Catheterization and Cardiovascular Diagnosis, 1990, 21, 185-194.	0.3	10
200	Issues of QCA validation:to the editor. Catheterization and Cardiovascular Diagnosis, 1994, 33, 97-98.	0.3	10
201	Micro stent I, initial results, and six months follow-up by quantitative coronary angiography. Catheterization and Cardiovascular Diagnosis, 1998, 43, 19-27.	0.3	10
202	Is there an effect of flat-panel-based imaging systems on quantitative coronary and vascular angiography?. Catheterization and Cardiovascular Interventions, 2006, 68, 561-566.	1.7	10
203	Coronary angiography enhancement for visualization. International Journal of Cardiovascular Imaging, 2009, 25, 657-667.	1.5	10
204	Texture analysis of ultrahigh field T <sub>2</sub> *â€weighted MR images of the brain: Application to Huntington's disease. Journal of Magnetic Resonance Imaging, 2014, 39, 633-640.	3.4	10
205	Myocardial stress perfusion-fibrosis imaging pattern in sarcoidosis, assessed by cardiovascular magnetic resonance imaging. International Journal of Cardiology, 2014, 172, 501-503.	1.7	10
206	Post-implantation shear stress assessment: an emerging tool for differentiation of bioresorbable scaffolds. International Journal of Cardiovascular Imaging, 2019, 35, 409-418.	1.5	10
207	Reliability and reproducibility of automated contour analysis in intravascular ultrasound images of femoropopliteal arteries. Ultrasound in Medicine and Biology, 1998, 24, 43-50.	1.5	9
208	Validation of a New Method for the Detection of Pathlines in Vascular X-ray Images. Investigative Radiology, 2004, 39, 524-530.	6.2	9
209	Gastric volume changes in response to a meal: Validation of magnetic resonance imaging versus the barostat. Journal of Magnetic Resonance Imaging, 2011, 34, 685-690.	3.4	9
210	Automatic radiographic quantification of hand osteoarthritis; accuracy and sensitivity to change in joint space width in a phantom and cadaver study. Skeletal Radiology, 2012, 41, 41-49.	2.0	9
211	Clinical validation of the new T―and Yâ€5hape models for the quantitative analysis of coronary bifurcations: An interobserver variability study. Catheterization and Cardiovascular Interventions, 2013, 81, E225-36.	1.7	9
212	Use of three-dimensional optical coherence tomography to verify correct wire position in a jailed side branch after main vessel stent implantation. EuroIntervention, 2011, 7, 528-529.	3.2	9
213	Metamodel-assisted mixed integer evolution strategies and their application to intravascular ultrasound image analysis. , 2008, , .		8
214	Quantitative evaluation of Compressed Sensing in MRI: Application to 7T time-of-flight angiography. , 2010, , .		8
215	Automated regional wall motion abnormality detection by combining rest and stress cardiac MRI: Correlation with contrastâ€enhanced MRI. Journal of Magnetic Resonance Imaging, 2011, 34, 270-278.	3.4	8
216	Assessment of endothelial shear stress in patients with mild or intermediate coronary stenoses using coronary computed tomography angiography: comparison with invasive coronary angiography. International Journal of Cardiovascular Imaging, 2017, 33, 1101-1110.	1.5	8

#	Article	IF	CITATIONS
217	Local Flow Patterns After Implantation of Bioresorbable Vascular Scaffold in Coronary Bifurcations ― Novel Findings by Computational Fluid Dynamics ―. Circulation Journal, 2018, 82, 1575-1583.	1.6	8
218	Effects of nifedipine on left ventricular performance in unstable angina pectoris during a follow-up of 48 hours. American Journal of Cardiology, 1986, 57, 1029-1033.	1.6	7
219	Inaccuracy of quantitative coronary arteriography when analyzed from S-VHS videotape. , 1996, 37, 32-38.		7
220	Objective Stenosis Quantification From Post-Stenotic Signal Loss in Phase-Contrast Magnetic Resonance Angiographic Datasets of Flow Phantoms and Renal Arteries. Magnetic Resonance Imaging, 1998, 16, 249-260.	1.8	7
221	MR OF THE HEART UNDER PHARMACOLOGIC STRESS. Cardiology Clinics, 1998, 16, 247-265.	2.2	7
222	Randomized, controlled trial of secondary prevention of coronary sclerosis in normocholesterolemic patients using pravastatin: two-year follow-up of the prevention of coronary sclerosis study. Current Therapeutic Research, 2001, 62, 473-485.	1.2	7
223	A New Approach to Contour Detection in X-Ray Arteriograms. Investigative Radiology, 2005, 40, 514-520.	6.2	7
224	Improved viscosity modeling in patients with type 2 diabetes mellitus by accounting for enhanced red blood cell aggregation tendency. Clinical Hemorheology and Microcirculation, 2010, 44, 303-313.	1.7	7
225	Non-parametric model selection for subject-specific topological organization of resting-state functional connectivity. Neurolmage, 2011, 56, 1453-1462.	4.2	7
226	Micro stent,â"¢ quantitative coronary angiography, and procedural results. , 1996, 38, 135-143.		6
227	The effect of DICOM on QCA and clinical trials. International Journal of Cardiovascular Imaging, 1998, 14, 7-12.	0.6	6
228	Time continuous segmentation of cardiac MR images using Active Appearance Motion Models. International Congress Series, 2001, 1230, 961-966.	0.2	6
229	A novel measurement technique to assess the effects of coronary brachytherapy in clinical trials. IEEE Transactions on Medical Imaging, 2002, 21, 1254-1263.	8.9	6
230	Automated Short-Axis Cardiac Magnetic Resonance Image Acquisitions. Investigative Radiology, 2004, 39, 747-755.	6.2	6
231	Combined magnitude and phaseâ€based segmentation of the cerebral cortex in 7T MR images of the elderly. Journal of Magnetic Resonance Imaging, 2012, 36, 99-109.	3.4	6
232	An automated tool for cortical feature analysis: Application to differences on 7 <scp>T</scp> esla <scp>T</scp> <sub>2</sub> <sup>*</sup> â€weighted images between young and older healthy subjects. Magnetic Resonance in Medicine, 2015, 74, 240-248.	3.0	6
233	Non-culprit coronary lesions in young patients have higher rates of atherosclerotic progression. International Journal of Cardiovascular Imaging, 2015, 31, 889-897.	1.5	6
234	In-stent fractional flow reserve variations and related optical coherence tomography findings: the FFR–OCT co-registration study. International Journal of Cardiovascular Imaging, 2018, 34, 495-502.	1.5	6

#	Article	IF	CITATIONS
235	Predictive value of the QFR in detecting vulnerable plaques in non-flow limiting lesions: a combined analysis of the PROSPECT and IBIS-4 study. International Journal of Cardiovascular Imaging, 2020, 36, 993-1002.	1.5	6
236	Automated Calibration in Vascular X-Ray Images Using the Accurate Localization of Catheter Marker Bands. Investigative Radiology, 2000, 35, 219-226.	6.2	6
237	Co-registration of fractional flow reserve and optical coherence tomography with the use of a three-dimensional angiographic roadmap: an opportunity for optimisation of complex percutaneous coronary interventions. EuroIntervention, 2013, 9, 889-889.	3.2	6
238	Influence of nifedipine on left ventricular perfusion and function in patients with unstable angina: Evaluation with radionuclide techniques. European Journal of Nuclear Medicine and Molecular Imaging, 1986, 11, 428-433.	2.1	5
239	Editorial comment. International Journal of Cardiovascular Imaging, 1995, 11, 209-210.	0.6	5
240	Influence of the selection of angiographic projections on the results of coronary angiographic follow-up trials. American Heart Journal, 1995, 130, 433-439.	2.7	5
241	The Influence of Angiographic Endpoints on the Outcome of Lipid Intervention Studies. Angiology, 1996, 47, 633-642.	1.8	5
242	End-diastolic and end-systolic volume from the left ventricular angiogram: how accurate is visual frame selection? Comparison between visual and semi-automated comnputer-assisted analysis. International Journal of Cardiovascular Imaging, 2003, 19, 259-266.	0.6	5
243	Computer-aided diagnosis via model-based shape analysis: cardiac MR and echo. International Congress Series, 2003, 1256, 1013-1018.	0.2	5
244	Optimization of Tryton Dedicated Coronary Bifurcation System With Coregistration of Optical Coherence Tomography and Fractional Flow Reserve. JACC: Cardiovascular Interventions, 2013, 6, e39-e40.	2.9	5
245	Anatomical and functional assessment of Tryton bifurcation stent before and after final kissing balloon dilatation: Evaluations by three-dimensional coronary angiography, optical coherence tomography imaging and fractional flow reserve. Catheterization and Cardiovascular Interventions, 2017, 90, E1-E10.	1.7	5
246	Angiography-Based 4-Dimensional Superficial Wall Strain and Stress: A New Diagnostic Tool in the Catheterization Laboratory. Frontiers in Cardiovascular Medicine, 2021, 8, 667310.	2.4	5
247	Comparison of left atrial strain measured by feature tracking computed tomography and speckle tracking echocardiography in patients with aortic stenosis. European Heart Journal Cardiovascular Imaging, 2021, 23, 95-101.	1.2	5
248	Automated Centerline Tracing in Coronary Angiograms. Machine Intelligence and Pattern Recognition, 1988, 7, 169-183.	0.2	5
249	Carina shift as a mechanism for side-branch compromise following main vessel intervention: insights from three-dimensional optical coherence tomography. Cardiovascular Diagnosis and Therapy, 2012, 2, 173-7.	1.7	5
250	Automatic border detection in IntraVascular UltraSound images for quantitative measurements of the vessel, lumen and stent parameters. International Congress Series, 2001, 1230, 916-922.	0.2	4
251	Active Appearance–Motion Models for fully automated endocardial contour detection in time sequences of echocardiograms. International Congress Series, 2001, 1230, 941-947.	0.2	4
252	Automatic stent border detection in intravascular ultrasound images. International Congress Series, 2003, 1256, 1111-1116.	0.2	4

#	Article	IF	CITATIONS
253	Stress cardiac magnetic resonance reveals myocardial perfusion impairment in asymptomatic diabetes mellitus type I, missed by the routine non-invasive evaluation. International Journal of Cardiology, 2013, 167, e167-e169.	1.7	4
254	Automatic detection of aorto-femoral vessel trajectory from whole-body computed tomography angiography data sets. International Journal of Cardiovascular Imaging, 2016, 32, 1311-1322.	1.5	4
255	Cardiovascular imaging of women and men visiting the outpatient clinic with chest pain or discomfort: design and rationale of the ARGUS Study. BMJ Open, 2020, 10, e040712.	1.9	4
256	Editorial comment: QCA and cine film exposure. , 1996, 39, 137-137.		3
257	A novel quantitative method for evaluating diffuse in-stent narrowing at follow-up angiography. Catheterization and Cardiovascular Interventions, 2001, 54, 309-317.	1.7	3
258	Influence of positional and angular variation of automatically planned short-axis stacks on quantification of left ventricular dimensions and function with cardiovascular magnetic resonance. Journal of Magnetic Resonance Imaging, 2005, 22, 754-764.	3.4	3
259	Topical issue: multimodality imaging in atherosclerosis. International Journal of Cardiovascular Imaging, 2016, 32, 1-3.	1.5	3
260	Cardiovascular imaging 2016 in the International Journal of Cardiovascular Imaging. International Journal of Cardiovascular Imaging, 2017, 33, 761-770.	1.5	3
261	Cardiovascular imaging 2017 in the International Journal of Cardiovascular Imaging. International Journal of Cardiovascular Imaging, 2018, 34, 833-848.	1.5	3
262	Endothelial shear stress and vascular remodeling in bioresorbable scaffold and metallic stent. Atherosclerosis, 2020, 312, 79-89.	0.8	3
263	Comparative effectiveness of coronary artery stenosis and atherosclerotic plaque burden assessment for predicting 30-day revascularization and 2-year major adverse cardiac events. International Journal of Cardiovascular Imaging, 2020, 36, 2365-2375.	1.5	3
264	One-year performance of biorestorative polymeric coronary bypass grafts in an ovine model: correlation between early biomechanics and late serial Quantitative Flow Ratio. European Journal of Cardio-thoracic Surgery, 2022, 61, 1402-1411.	1.4	3
265	Angiography and digital radiography. Current Opinion in Cardiology, 1989, 4, 853-862.	1.8	2
266	In vivo comparison of different quantitative edge detection systems used for measuring coronary arterial diameters. Catheterization and Cardiovascular Diagnosis, 1995, 34, 81-81.	0.3	2
267	Cardiovascular imaging 2010 in the International Journal of Cardiovascular Imaging. International Journal of Cardiovascular Imaging, 2011, 27, 309-319.	1.5	2
268	Cardiovascular imaging 2013 in the International Journal of Cardiovascular Imaging. International Journal of Cardiovascular Imaging, 2014, 30, 683-695.	1.5	2
269	Population based ultrasonographic screening of abdominal aortic aneurysms. International Journal of Cardiovascular Imaging, 2016, 32, 1605-1607.	1.5	2
270	Cardiovascular imaging 2019 in the International Journal of Cardiovascular Imaging. International Journal of Cardiovascular Imaging, 2020, 36, 769-787.	1.5	2

#	Article	IF	CITATIONS
271	Three-Dimensional Reconstruction of Myocardial Contrast Perfusion from Biplane Cineangiograms. Machine Intelligence and Pattern Recognition, 1988, 7, 155-168.	0.2	2
272	A Model for the Modulation Transfer Function of Cardiovascular X-ray Systems. Investigative Radiology, 1996, 31, 161-172.	6.2	2
273	Heart Team risk assessment with angiographyâ€derived fractional flow reserve determining the optimal revascularization strategy in patients with multivessel disease: Trial design and rationale for the DECISION QFR randomized trial. Clinical Cardiology, 2022, , .	1.8	2
274	Overestimation of small vessel sizes by QCA. Catheterization and Cardiovascular Diagnosis, 1995, 36, 25-26.	0.3	1
275	On the statistical modelling of coronary arteriographic data: dynamics of coronary atherosclerosis related to systemic and focal parameters. , 1997, 16, 2829-2841.		1
276	Recent Advances in MRI Based Volumetry and Morphometry for AD Diagnosis in Human. Current Medical Imaging, 2011, 7, 34-42.	0.8	1
277	Introduction to QCA, IVUS and OCT in interventional cardiology. International Journal of Cardiovascular Imaging, 2011, 27, 153-154.	1.5	1
278	QCA editorial. International Journal of Cardiovascular Imaging, 2011, 27, 155-156.	1.5	1
279	Stress perfusion–fibrosis cardiac magnetic resonance detects early heart involvement in young asymptomatic, homozygous familial hyperlipidemia with normal routine non-invasive evaluation. International Journal of Cardiology, 2013, 168, 4570-4572.	1.7	1
280	Response to Letters Regarding Article, "Comparison of Clinical Interpretation With Visual Assessment and Quantitative Coronary Angiography in Patients Undergoing Percutaneous Coronary Intervention in Contemporary Practice: The Assessing Angiography (A2) Project― Circulation, 2013, 128, e463-4.	1.6	1
281	An Objective Method to Optimize the MR Sequence Set for Plaque Classification in Carotid Vessel Wall Images Using Automated Image Segmentation. PLoS ONE, 2013, 8, e78492.	2.5	1
282	Editor's note September 2014. International Journal of Cardiovascular Imaging, 2014, 30, 1205-1206.	1.5	1
283	Angiography-derived physiology guidance vs usual care in an All-comers PCI population treated with the healing-targeted supreme stent and Ticagrelor monotherapy: PIONEER IV trial design. American Heart Journal, 2022, 246, 32-43.	2.7	1
284	Comment on "editorial comment―from masakiyo nobuyoshi, m.d.,cathet cardiovasc diagn33:156(1994). Catheterization and Cardiovascular Diagnosis, 1995, 34, 372-372.	0.3	0
285	Editor's comments. International Journal of Cardiovascular Imaging, 1995, 11, 143-144.	0.6	0
286	769-1 The Influence of Pravastatin on Progression and Regression of Coronary Atherosclerosis in Men with Normal or Mildly Raised Serum Cholesterol. Results of the Regression Growth Evaluation Statin Study (REGRESS). Journal of the American College of Cardiology, 1995, 25, 281A.	2.8	0
287	Value of angiotensin converting enzyme inhibition in patients with myocardial infarction, aggressively treated with thrombolysis or acute PTCA. Journal of the American College of Cardiology, 1996, 27, 248-249.	2.8	0
288	Intravascular ultrasound. R. Erbel, J.R.T.C. Roelandt, J. Ge, G. Goerge, editors International Journal of Cardiovascular Imaging, 1998, 14, 71-71.	0.6	0

#	Article	IF	CITATIONS
289	How deterministic can the angiogram be?. Catheterization and Cardiovascular Interventions, 1999, 48, 446-446.	1.7	Ο
290	Diagnostic Imaging in Clinical Cardiology. João A.C. Lima, editor. International Journal of Cardiovascular Imaging, 2000, 16, 67-67.	0.6	0
291	Myocardial Viability. 2nd Completely Revised Version. A.E. Iskandrian, E.E. van der Wall, editors International Journal of Cardiovascular Imaging, 2000, 16, 125-125.	0.6	0
292	Title is missing!. International Journal of Cardiovascular Imaging, 2001, 17, 77-77.	0.6	0
293	Strategic collaboration with the European Society of Cardiovascular Radiology (ESCR). International Journal of Cardiovascular Imaging, 2006, 22, 599-599.	1.5	0
294	Eureka?. Radiology, 2011, 259, 610-611.	7.3	0
295	Cardiovascular imaging 2011 in the International Journal of Cardiovascular Imaging. International Journal of Cardiovascular Imaging, 2012, 28, 439-451.	1.5	0
296	Editor's note August, 2013. International Journal of Cardiovascular Imaging, 2013, 29, 1201-1202.	1.5	0
297	Cardiovascular imaging 2012 in the International Journal of Cardiovascular Imaging. International Journal of Cardiovascular Imaging, 2013, 29, 725-736.	1.5	0
298	Editor's note October, 2013. International Journal of Cardiovascular Imaging, 2013, 29, 1655-1655.	1.5	0
299	Editor's note January 2014. International Journal of Cardiovascular Imaging, 2014, 30, 1-7.	1.5	0
300	Editor's note July 2014. International Journal of Cardiovascular Imaging, 2014, 30, 991-991.	1.5	0
301	Editor's note March 2014. International Journal of Cardiovascular Imaging, 2014, 30, 467-467.	1.5	0
302	Editor's note February 2015. International Journal of Cardiovascular Imaging, 2015, 31, 221-223.	1.5	0
303	Cardiovascular imaging 2015 in the International Journal of Cardiovascular Imaging. International Journal of Cardiovascular Imaging, 2016, 32, 697-709.	1.5	0
304	Cardiovascular imaging 2017 in the International Journal of Cardiovascular Imaging. International Journal of Cardiovascular Imaging, 2018, 34, 1003-1003.	1.5	0
305	Topical issue: advanced imaging and endovascular treatment in pulmonary artery diseases. International Journal of Cardiovascular Imaging, 2019, 35, 1405-1406.	1.5	0
306	Cardiovascular imaging 2018 in the International Journal of Cardiovascular Imaging. International Journal of Cardiovascular Imaging, 2019, 35, 1175-1188.	1.5	0

#	Article	IF	CITATIONS
307	Introduction topical issue on CT plaque burden. International Journal of Cardiovascular Imaging, 2020, 36, 2301-2303.	1.5	0
308	Editor's note February 2020. International Journal of Cardiovascular Imaging, 2020, 36, 767-767.	1.5	0
309	Cardiovascular imaging 2020 in the international journal of cardiovascular imaging: the 10 most downloaded papers in the year 2020. International Journal of Cardiovascular Imaging, 2021, 37, 1105-1106.	1.5	0
310	Editor's note to the June 2021 issue. International Journal of Cardiovascular Imaging, 2021, 37, 1799-1800.	1.5	0
311	Editor's Note to the July 2021 issue. International Journal of Cardiovascular Imaging, 2021, 37, 2093-2094.	1.5	0
312	Increased 2020 impact factor for Int Journal Cardiovascular Imaging: 2.357. International Journal of Cardiovascular Imaging, 2021, 37, 2345-2346.	1.5	0
313	Editor's note to the September 2021 issue. International Journal of Cardiovascular Imaging, 2021, 37, 2589-2589.	1.5	0
314	Editor's choice to the October 2021 issue. International Journal of Cardiovascular Imaging, 2021, 37, 2801-2802.	1.5	0
315	Editor's choice to the november 2021 issue. International Journal of Cardiovascular Imaging, 2021, 37, 3127-3128.	1.5	0
316	Evaluating Visualisations and Automatic Warning Cues for Visual Search in Vascular Images. , 2012, , 68-83.		0
317	THE FUSION OF THREE-DIMENSIONAL QUANTITATIVE CORONARY ANGIOGRAPHY AND INTRACORONARY IMAGING FOR CORONARY INTERVENTIONS. Series in Computer Vision, 2014, , 151-173.	0.1	0
318	Quantitative Assessment of the Presence of a Single Leg Separation in Björk-Shiley Convexoconcave Prosthetic Heart Valves. Investigative Radiology, 1997, 32, 540-549.	6.2	0
319	Editor's Choice to the December 2021 issue. International Journal of Cardiovascular Imaging, 2021, 37, 3371-3372.	1.5	0
320	Editor's choice to the January 2022 issue. International Journal of Cardiovascular Imaging, 2022, 38, 1-3.	1.5	0
321	Global longitudinal strain (GLS). International Journal of Cardiovascular Imaging, 2022, 38, 269-270.	1.5	0
322	Recovery of right ventricular function and strain. International Journal of Cardiovascular Imaging, 2022, 38, 491-492.	1.5	0
323	Editor's Choice to the April 2022 issue. International Journal of Cardiovascular Imaging, 0, , 1.	0.6	0
324	Editor's choice to the May 2022 issue. International Journal of Cardiovascular Imaging, 2022, 38, 915.	0.6	0